SPECTRUM OF ENGINEERING SCIENCES
ISSN (E) 3007-3138 (P) 3007-312X VOLUME 4, ISSUE 3, 2026

QUANTUM MATERIALS ENGINEERING FOR NEXT-GENERATION ELECTRONICS: LINKING ELECTRONIC STRUCTURE, DEFECT CHEMISTRY, AND NANOSCALE TRANSPORT IN FUNCTIONAL MATERIALS

Umar Shahzab*[1], Amina[2]

*[1]*Department of Physics, Islamia University Bahawalpur, Pakistan*
[2]*Department of Physics, Bacha Khan University Charsadda, Pakistan*
[2]*Energy Institute, Istanbul Technical University, Türkiye*

*[1]umarshahzabamjad786@gmail.com, [2]dramina.faculty@bkuc.edu.pk

DOI: https://doi.org/10.5281/zenodo.24079893

Keywords
quantum materials; defect chemistry; electronic structure; nanoscale transport; topological insulators; moiré superlattices; spin qubits; high-entropy oxides; DFT-NEGF; next-generation electronics.

Article History
Received: 01 January 2026
Accepted: 16 March 2026
Published: 31 March 2026

Copyright @Author
Corresponding Author: *
Umar Shahzab

Abstract

The relentless scaling of silicon-based complementary metal-oxide-semiconductor (CMOS) technology is approaching fundamental physical limits, including short-channel effects, quantum tunneling leakage, and excessive Joule heating. Quantum materials encompassing two-dimensional van der Waals heterostructures, topological insulators, Dirac and Weyl semimetals, complex oxides, and high-entropy phases offer transformative paradigms for next-generation electronics by exploiting quantum degrees of freedom such as spin, valley index, and topological surface states. This review establishes a unified framework linking three interconnected domains: electronic structure, defect chemistry, and nanoscale transport dynamics. We examine Kröger-Vink defect equilibria in functional oxides, strain-defect coupling at dislocations, thermal tuning of anti-site defects in magnetic topological materials, and entropy-stabilized defect landscapes in high-entropy oxides. Electronic structure modulation through band topology, correlated moiré physics, and interfacial Rashba coupling is analyzed alongside quantum transport formalisms, including density functional theory coupled with non-equilibrium Green's functions (DFT-NEGF), topological protection mechanisms, spin qubit dephasing, and terahertz-driven ultrafast dynamics. Next-generation device architectures are discussed, including spintronic logic and memory, silicon and germanium hole spin-qubit integration, and defect-mediated catalytic electronics. Finally, we address emerging bottlenecks in deterministic defect synthesis, machine-learning-assisted material discovery, and interfacial strain management for CMOS integration. By redefining defects as deterministic design tools rather than unwanted anomalies, this review provides a rational pathway toward post-CMOS microelectronics, spintronic memory, and quantum hardware.

1. INTRODUCTION

The continuous scaling of conventional silicon-based complementary metal-oxide-semiconductor (CMOS) field-effect transistors is confronting fundamental physical limits. As feature sizes shrink into the sub-10 nanometer regime, classical architectures suffer from severe short-channel effects, elevated source-to-drain quantum tunneling leakage, parasitic interface trap states, and excessive Joule heating (Mengesha &

Nagessar, 2025). To surpass these scaling constraints, condensed matter physics and materials science have shifted toward quantum materials a broad class of systems where strong electron-electron correlations, non-trivial wave function topology, spin-orbit coupling, and low-dimensional quantum confinement dictate macroscopic behavior (Chen et al., 2025).

Quantum materials, comprising two-dimensional (2D) van der Waals heterostructures, topological insulators (TIs), Dirac and Weyl semimetals, complex oxides, and high-entropy phases, offer operational paradigms for next-generation information processing. Rather than relying solely on charge presence, these functional platforms leverage quantum degrees of freedom such as electron spin, valley index, topological surface states, and phase transitions to achieve ultra-low-power, high-speed computation (Pal et al., 2023).

1.2 The Triad of Electronic Structure, Defect Chemistry, and Nanoscale Transport

Realizing practical quantum devices requires a unified understanding of three interconnected domains: electronic structure, defect chemistry, and nanoscale transport dynamics (Zhang et al., 2025).

The electronic band structure defines fundamental parameters such as carrier effective mass, spin-orbit splitting, topological invariants, and state densities. Defect chemistry dictates how point defects, vacancies, anti-site substitutions, and extended structural boundaries form, interact, and redistribute under thermal and chemical driving forces. Nanoscale transport governs how charge, spin, and heat move through these perturbed potential landscapes under external bias, magnetic fields, or optical excitation (Smalley et al., 2026).

Historically, crystal defects were viewed as unwanted anomalies that degrade device performance by inducing carrier scattering and phase dephasing. Modern quantum materials engineering redefines point defects and structural boundaries as deterministic design tools (Zhang et al., 2026). Local strain fields, vacancy complexes, and anti-site defects can locally reshape the electronic density of states, break local inversion symmetry, induce localized magnetic order, and alter topological phase stability. Understanding this triad enables the rational design of functional materials tailored for post-CMOS microelectronics, spintronic memory, and quantum hardware (Guo et al., 2019).

IEER
Institute for Excellence in Education & Research

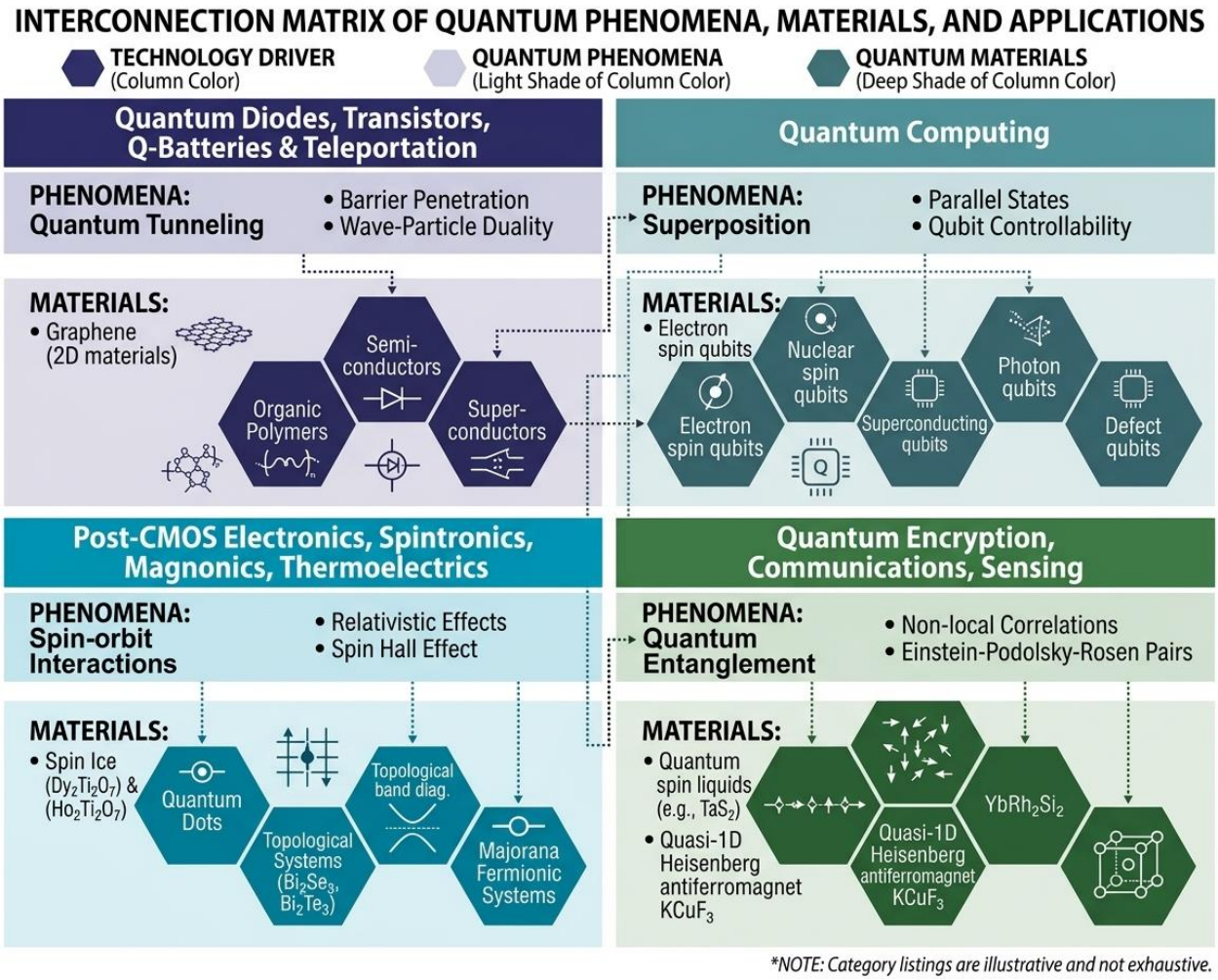


Figure 1: Interconnection Matrix of Quantum Phenomena, Functional Materials, and Emerging Technological Applications

2. Defect Thermodynamics and Kröger-Vink Formalisms in Functional Materials

2.1 Kröger-Vink Defect Equilibria in Complex Oxides

Defect thermodynamics provides a quantitative framework for engineering electrical conductivity, carrier species, and non-stoichiometry in functional oxides. Point defect equilibria are modeled using Kröger-Vink notation, where defect charges are defined relative to the neutral host lattice site. In p-type delafossite semiconductors like $CuCoO_2$, intrinsic defect formation during high-temperature or hydrothermal synthesis controls hole conduction (Youssef & Yildiz, 20012). The oxidation of cuprous ions (Cu^{+}) to cupric ions (Cu^{2+}) yields acceptor-like copper vacancies (V_{Cu}') and electron holes ($h^{\cdot}$):

$$\frac{1}{2}O_2(g) \rightleftharpoons O_O^{\times} + V_{Cu}' + h^{\cdot}$$

Conversely, Co-site reduction (Co^{3+} to Co^{2+}) leads to oxygen vacancy ($V_O^{\cdot\cdot}$) formation accompanied by electron (e') generation, establishing a competing defect equilibrium:

$$O_O^{\times} \rightleftharpoons \frac{1}{2}O_2(g) + V_O^{\cdot\cdot} + 2e'$$

$$2Co_{Co}^{\times} + O_O^{\times} \rightleftharpoons \frac{1}{2}O_2(g) + V_O^{\cdot\cdot} + 2Co_{Co}'$$

These defect reactions determine whether the material behaves as a p-type hole conductor, an n-type electronic semiconductor, or a mixed ionic-electronic conductor (MIEC) (Kemp, 2023).

2.2 Strain-Defect Coupling at Dislocations and Space-Charge Regions

In functional oxide heterostructures, such as epitaxial ferromagnetic metallic $La_{0.7}Sr_{0.3}MnO_3$ (LSMO) thin films grown on insulating $LaAlO_3$ (LAO), lattice mismatch generates structural strain fields. Strain relaxation occurs via networks of misfit dislocations (MDs). The non-uniform stress field surrounding a dislocation core breaks localized thermodynamic equilibrium, establishing a driving force for point defect segregation (Uberuaga et al., 2019).

In regions of localized tensile strain near the dislocation core, the formation enthalpy of oxygen vacancies decreases. The corresponding point defect reaction couples oxygen loss directly to cation valence reduction:

$$O_O^{\times} + 2Mn_{Mn}^{\times} \rightleftharpoons \frac{1}{2}O_2(g) + V_O^{\cdot\cdot} + 2Mn_{Mn}{}'$$

where $Mn_{Mn}^{\times}$ represents the nominal host manganese valence state and $Mn_{Mn}{}'$ denotes reduced Mn^{3+} cations. Each doubly charged oxygen vacancy ($V_O^{\cdot\cdot}$) releases two electrons into localized manganese $3d\ e_g$ states, reducing smaller Mn^{4+} cations (ionic radius $r \approx 0.610$ Å) to larger Mn^{3+} cations ($r \approx 0.645$ Å) (Murthy et al., 2016). This chemical reduction induces a local chemical expansion of approximately 6%, relaxing localized tensile stress and lowering the system's elastic energy. Accumulation of positive $V_O^{\cdot\cdot}$ species at dislocation cores generates localized space-charge potential barriers across length scales ranging from tens to hundreds of nanometers, producing insulating boundary regions within a metallic matrix (Chen et al., 2019).

2.3 Thermal Tuning of Anti-Site Defects in Magnetic Topological Materials

In magnetic topological materials like $MnSb_2Te_4$, thermodynamic growth conditions directly control the anti-site defect density, dictating both the magnetic ground state and topological surface spectrum. Single crystals grown at 620 °C yield near-ideal stoichiometry and order antiferromagnetically at a Néel temperature $T_N = 19$ K. Increasing the growth temperature to 625 °C favors the formation of manganese-rich anti-site defects ($Mn_{Sb}^{\cdot}$), where Mn^{2+} cations substitute onto Sb^{3+} lattice sites within $[Te - Sb - Te - Mn - Te - Sb - Te]$ septuple layers (Hu et al., 2024).

These anti-site defects mediate ferromagnetic exchange coupling across van der Waals gaps, switching the low-temperature magnetic ordering from antiferromagnetic to ferrimagnetic with a Curie temperature $T_C = 24$ K. Density Functional Theory (DFT) calculations confirm that these localized anti-site defects alter spin-orbit splitting at the Brillouin zone center (Γ-point), demonstrating how synthesis temperature can be used to control magnetic and topological states (Chen et al., 2026).

2.4 High-Entropy Oxides (HEOs) and Entropy-Stabilized Defect Landscapes

High-entropy oxides (HEOs) incorporate five or more cation species in near-equimolar ratios on a single sublattice, introducing configurational entropy stabilization to functional ceramics. The phase stability of HEOs is driven by the configurational entropy of mixing:

$$S_{config} = -R\sum_{i=1}^{N} x_i \ln x_i$$

where R is the universal gas constant and x_i is the mole fraction of cation species i (Lyu et al., 2026). In rare-earth high-entropy oxides (RE-HEOs), high configurational entropy suppresses long-range cation ordering while stabilizing large concentrations of point defects, particularly oxygen vacancies. In ceria-based RE-HEO systems, oxygen vacancies modulate energy gaps between oxygen $2p$ and cerium $4f/5d$ orbitals. The local lattice distortion induced by cation size mismatch lowers the $V_O^{\cdot\cdot}$ formation energy, yielding high oxygen mobility and structural stability under extreme thermal conditions (> 800 °C) (Sun et al., 2026).

Table 1: Defect Reactions, Kröger-Vink Formalisms, and Physical Impacts in Functional Materials

Material System	Defect Reaction / Formalism	Primary Defect Species	Physical Impact on Electronic and Transport Properties
Delafossite $CuCoO_2$	$\frac{1}{2}O_2 \rightleftharpoons O_O^{\times} + V_{Cu}' + h^{\cdot}$	$O_O^{\times} \rightleftharpoons \frac{1}{2}O_2 + V_O^{\cdot\cdot} + 2e'$ | V_{Cu}' (Acceptor), $V_O^{\cdot\cdot}$ (Donor)	Controls p-type hole conductivity; dictates charge-transfer resistance (R_{ct}) during electrocatalytic operations.
Epitaxial LSMO / LAO	$O_O^{\times} + 2Mn_{Mn}^{\times} \rightleftharpoons \frac{1}{2}O_2 + V_O^{\cdot\cdot} + 2Mn_{Mn}'$ | $V_O^{\cdot\cdot}$, Mn_{Mn}' (Mn^{3+})	Drives 6% local chemical expansion at dislocation cores; establishes 10–100 nm space-charge potential barriers (Bak et al., 2024).
Topological $MnSb_2Te_4$	$Mn_{interstitial} + V_{Sb}' \rightleftharpoons Mn_{Sb}^{\cdot} + e'$ | $Mn_{Sb}^{\cdot}$ Anti-site defect	Switches magnetic order from Antiferromagnetic (19 K) to Ferrimagnetic (24 K); alters topological Dirac gap.
Rare-Earth High-Entropy Oxides	$S_{config} = -R\sum x_i \ln x_i$ $Ce_{Ce}^{\times} + O_O^{\times} \rightleftharpoons Ce_{Ce}' + \frac{1}{2}O_2 + V_O^{\cdot\cdot}$ | $V_O^{\cdot\cdot}$, Ce_{Ce}' (Ce^{3+})	Stabilizes oxygen vacancies; tunes 2p–4f and 2p–5d electronic band gaps; imparts thermal resilience > 800 °C (Squires et al., 2026).

3. Electronic Structure Modulation: Band Topology, Correlation Effects, and Moiré Physics

3.1 Band Structure and Fermi-Level Engineering in Low-Dimensional Materials

Two-dimensional (2D) crystals provide a versatile platform for electronic structure engineering due to their high mechanical flexibility and sensitivity to external fields. Applied mechanical strain alters orbital overlap integrals, shifting energy bands across the Brillouin zone (Adak et al., 2024). In monolayer octagonal-nitrogen (ON) and van der Waals (vdW) heterostructures, applying biaxial tensile strain or a perpendicular electric field reduces the conduction-to-valence band gap, inducing an insulator-to-metal transition. Similarly, lithographic patterning of graphene nanoribbons introduces lateral spatial confinement, opening a width-dependent band gap in an otherwise gapless semimetal 9 Kim et al., 2023).

In 2D transition metal carbides and nitrides (MXenes), such as $Ti_3C_2T_x$ (where T_x represents surface terminations like −O, −OH, or −F), the Fermi-level density of states is governed by surface stoichiometry. Although single-layer MXene flakes exhibit metallic conductivity, ambient degradation causes selective edge oxidation (Abbas et al., 2020). The formation of titanium oxide sub-phases introduces scattering centers, driving an initial exponential drop followed by a linear decline in carrier mobility. Additionally, thermal transport in MXenes involves a coupled electron-phonon mechanism where acoustic phonons contribute significantly to heat dissipation across van der Waals channels despite the material's metallic nature (Yao et al., 2020).

3.2 Correlated Electron States in Moiré Superlattices

Superimposing two 2D atomic layers with a rotational twist angle (θ) forms a long-period moiré superlattice. This spatial modulation creates a periodic superlattice potential that flattens the kinetic energy bandwidth (W) of delocalized electrons. When the bandwidth W becomes much smaller than the on-site Coulomb repulsion energy (U), electron correlations dominate system behavior (Huang et al., 2022).

At "magic twist angles" (e.g., $\theta \approx 1.08°$ in twisted bilayer graphene), flat electronic bands emerge near the neutrality point. Electrostatic gating to fractional band fillings isolates electrons within individual moiré unit cells, driving the system into a Mott-like correlated insulating state (Shimazaki et al., 2020). Doping away from these correlated insulating states destabilizes the localized electron configuration, inducing a transition into unconventional superconducting phases. Moiré engineering thus provides a controllable solid-state

platform for exploring strongly correlated electron dynamics (Campbell et al., 2022).

3.3 Interfacial Quantum States and Rashba Coupling in Oxide Heterostructures

Interfacial confinement at oxide heterostructures can generate electronic states absent in the constituent bulk materials. A classic example occurs at the interface between the band insulators $LaAlO_3$ (LAO) and $SrTiO_3$ (STO) (Caviglia et al., 2010). Exceeding a critical LAO film thickness of four unit cells triggers an electronic reconstruction transferring charge from the LAO surface to the interface to prevent electrostatic potential divergence (polar catastrophe). This charge transfer forms a quasi-two-dimensional electron gas (2DEG) confined within a few nanometers of the STO surface (Lesne et al., 2016).

The LAO/STO 2DEG exhibits high carrier mobility alongside strong, gate-tunable Rashba spin-orbit coupling. Spatial inversion symmetry breaking splits the spin sub-bands, enabling efficient charge-to-spin conversion via the inverse Rashba-Edelstein effect (IREE). Depositing ultra-thin reactive metal overlayers onto the LAO surface scavenges lattice oxygen, creating interfacial oxygen vacancies ($V_O^{\cdot\cdot}$) that modulate 2DEG carrier density and charge-to-spin conversion efficiency (Cheng et al., 2017).

4. Nanoscale Quantum Transport Dynamics and Transient Physics

4.1 First-Principles Non-Equilibrium Green's Function (NEGF) Transport Modeling

To model quantum transport in atomic-scale devices, standard semiclassical Boltzmann transport theory must be replaced by quantum formalisms combining Density Functional Theory with Non-Equilibrium Green's Functions (DFT-NEGF) (Pourfath, 2014). The retarded Green's function $\mathbf{G}(\mathrm{E})$ of a scattering region connected to semi-infinite source and drain leads is given by:

$$\mathbf{G}(\mathrm{E}) = [(\mathrm{E} + \mathrm{i}\eta)\mathbf{S} - \mathbf{H} - \mathbf{\Sigma}_{\mathrm{S}}(\mathrm{E}) - \mathbf{\Sigma}_{\mathrm{D}}(\mathrm{E})]^{-1}$$

where $\mathbf{H}$ and $\mathbf{S}$ are the Hamiltonian and overlap matrices of the central device region, and $\mathbf{\Sigma}_{\mathrm{S,D}}(\mathrm{E})$ are the self-energy matrices describing open-boundary coupling to the leads. The quantum transmission function $\mathrm{T}(\mathrm{E})$ is calculated using the Landauer-Büttiker formula:

$$\mathrm{T}(\mathrm{E}) = \mathrm{Tr}\left[\mathbf{\Gamma}_{\mathrm{S}}(\mathrm{E})\mathbf{G}(\mathrm{E})\mathbf{\Gamma}_{\mathrm{D}}(\mathrm{E})\mathbf{G}^{\dagger}(\mathrm{E})\right]$$

where $\mathbf{\Gamma}_{\mathrm{S,D}} = \mathrm{i}\left(\mathbf{\Sigma}_{\mathrm{S,D}} - \mathbf{\Sigma}_{\mathrm{S,D}}^{\dagger}\right)$ denote the broadenings.

DFT-NEGF modeling illustrates how specific defect configurations modulate energy-dependent transmission profiles (Wang, 2013). In polycrystalline graphene, grain boundaries (GBs) act as line defects consisting of repeating pentagon-heptagon carbon ring pairs. Quantum transport simulations demonstrate that GB transmission is highly anisotropic: transport perpendicular to the GB is strongly attenuated by destructive quantum interference, whereas transport parallel to the boundary remains highly conductive (Rungger et al., 2020).

Controlled nitrogen ion implantation introduces substitutional nitrogen defect centers. When arranged in nanoscale constrictions, these defects induce quantum interference that modulates transmission, enabling electron confinement over tens of nanometers (Szabó et al., 2016). Chemisorption of individual atoms such as binding a single selenium atom to pristine graphene breaks local A–B sublattice symmetry. Spatially resolved local density of states (LDOS) maps around the chemisorbed selenium atom display Friedel-like oscillations with characteristic quantum phase shifts, providing a direct measurement of graphene's non-trivial Berry phase (Ho et al., 2020).

4.2 Topological Protection, Spin-Momentum Locking, and Domain Boundary Inhomogeneities

Topological Quantum Materials (TQMs) including topological insulators (Bi_2Se_3, Bi_2Te_3) and Dirac or Weyl semimetals (Cd_3As_2, TaAs, NbP) host boundary states protected by time-reversal or crystalline symmetries. Strong spin-orbit coupling locks carrier spin perpendicular to momentum ($\mathbf{k}$), establishing spin-momentum locking. Because elastic backscattering from $\mathbf{k}$ to $-\mathbf{k}$ requires a complete spin reversal, scattering from non-magnetic impurities is suppressed, yielding high carrier mobility even in defective crystals (Chen et al., 2018).

In magnetic topological conductors, spatial magnetic inhomogeneities introduce transport

complexity. Spatially varying magnetic domain configurations generate local anomalous Hall conductivities $\sigma_{xy}(\mathbf{r})$ that reverse sign across domain walls (Weber et al., 2024). The macroscopic Hall transport tensor $\bar{\boldsymbol{\sigma}}$ under spatial variations is bounded by Hashin-Shtrikman limits:

$$\sigma_h^{lower} \leq \bar{\sigma}_{xy} \leq \sigma_h^{upper}$$

Domain-wall nucleation at local defect sites distorts macroscopic Hall resistance measurements, producing asymmetric dips and hysteretic signatures. These classical inhomogeneity-induced transport features can mimic signatures of the Topological Hall Effect (THE) often misattributed to skyrmion spin textures highlighting the need to distinguish intrinsic Berry curvature contributions from defect-driven spatial transport fluctuations (Kleemann, 2007).

4.3 Quantum Dot Dynamics, Spin Qubits, and Charge Noise Dephasing

Group-IV semiconductor heterostructures, including strained planar Germanium (Ge) quantum wells and Fully Depleted Silicon-on-Insulator (FD-SOI) platforms, serve as physical architectures for scalable quantum logic. Spin qubits based on hole states in Germanium double quantum dots (DQDs) exploit strong intrinsic spin-orbit coupling, enabling fast, electrical gate-driven spin manipulation without micro-magnets (Yoneda et al., 2018).

However, interface traps and dielectric charge noise introduce $1/f$ electric field fluctuations that cause spin dephasing. Quantum device simulations incorporating interface trap noise models indicate that optimizing gate geometries and dielectric interfaces reduces charge noise, yielding hole-spin dephasing times $T_2^* = 27.68\ \mu s$ and two-qubit gate fidelities reaching 99.81% (Hu & Das Sarma, 2006). Advanced CMOS-compatible 22FDX FD-SOI architectures enable double quantum dot configurations operating without individual barrier control gates, simplifying circuit layouts while maintaining spin manipulation speeds ($1\ \mu s$) and Hahn-echo coherence times ($T_2 = 40\ \mu s$) (Culcer et al., 2009).

4.4 Out-of-Equilibrium Ultrafast Transport via Terahertz STM

Steady-state transport measurements cannot resolve ultrafast phase dynamics or non-equilibrium electronic transitions. Terahertz Scanning Tunneling Microscopy (THz-STM) overcomes this limitation by coupling single-cycle, sub-picosecond THz voltage pulses into an atomic STM junction. The transient electric field pulse drives junction electrons far out of equilibrium on femtosecond timescales (Shi et al., 2020).

To model transient dynamics, atomistic DFT-NEGF calculations utilize an auxiliary-mode expansion method. Eigendecomposition of the lead self-energy matrices allows real-time tracking of transient current pulses across nanoscale constrictions. Applying this framework to single-atom gold junctions, spin-polarized hydrogen on graphene, and nanoribbons resolves sub-picosecond quantum transport mechanisms, providing a theoretical foundation for atomic-scale, terahertz-driven electronic switching (Kužel & Němec, 2020).

Table 2: Comparative Analysis of Quantum Material Platforms for Next-Generation Electronics

Material Class	Platform Examples	Key Transport Mechanisms	Major Functional Applications	Critical Engineering Bottlenecks
Topological Insulators & Semimetals	Bi_2Se_3, Bi_2Te_3, TaAs, Cd_3As_2	Spin-momentum locked Dirac surface states; suppressed backscattering; linear dispersion.	Low-power spintronics, topological quantum gates, high-mobility channels.	Native point defects generating bulk conduction that masks surface state transport.
2D Van der Waals Heterostructures	Graphene, MoS_2, MXenes ($Ti_3C_2T_x$)	Ballistic sub-nm transport; strain-tunable bandgaps; high mechanical flexibility.	Ultra-scaled FETs, flexible optoelectronics, transparent electrodes.	Edge oxidation degradation, contact resistance, scalable defect-free synthesis.
Correlated Moiré Superlattices	Twisted Bilayer Graphene, TMD Moiré layers	Bandwidth compression ($W \ll U$); flat-band formation; Mott-like correlated states.	Switchable phase-change logic, unconventional superconductivity simulators.	High sensitivity to twist-angle spatial heterogeneity and local strain.
Complex Oxide Interfaces	$LaAlO_3$/ $SrTiO_3$ (LAO/STO)	Polar catastrophe induced 2DEG; gate-tunable Rashba spin-orbit coupling.	Spin-orbit torque (SOT) logic, reconfigurable interfacial interconnects.	Defect-induced space-charge layers; ionic oxygen drift under sustained electric bias.
Group-IV Quantum Dots	Strained Planar Ge, FD-SOI Silicon	Electric-field driven hole spin manipulation; CMOS process compatibility.	Scalable spin-qubit processors, room-temperature single-electron transistors.	1/f charge noise from dielectric interface traps causing spin dephasing.

5. Next-Generation Device Architectures and Functional Applications

5.1 Spintronic Logic, Memory, and Topological Quantum Devices

Integrating topological materials into spintronic architectures enables non-volatile logic and memory devices operating below traditional thermal dissipation limits. Leveraging the spin Hall angle in topological insulators (Bi_2Se_3) or Rashba-split oxide 2DEGs (LAO/STO) enables current-induced spin-orbit torque (SOT) switching of adjacent perpendicular ferromagnets (Tasiu et al., 2025).

When charge current flows through spin-momentum locked surface states, it generates a transverse spin current that exerts a torque on an adjacent ferromagnetic layer. This torque flips the ferromagnet's magnetization without requiring current passage through an insulating barrier, suppressing Joule heating. Additionally, skyrmion-based memory architectures utilize non-trivial chiral spin textures to store binary data, relying on topological protection to achieve low depinning current densities (Banerjee et al., 2025).

5.2 Silicon and Germanium Hole Spin-Qubit Integration

Scaling from individual quantum dots to dense qubit arrays requires minimizing control wiring while preserving quantum coherence. Planar Germanium quantum wells grown on Silicon-Germanium (SiGe) substrates provide a path forward, as Germanium's weak hyperfine

interaction with host nuclei suppresses nuclear-spin-induced dephasing (Fang et al., 2023).

To simplify wiring in multi-qubit integrated circuits, standardized cell designs have been implemented using commercial Fully Depleted Silicon-on-Insulator (FD-SOI) technology nodes, such as 22FDX. Eliminating individual inter-dot barrier control gates simplifies fabrication while allowing precise inter-dot coupling control using global top gates. This architectural approach enables the integration of single-electron transistors and multi-qubit arrays within established silicon manufacturing infrastructure (Liu et al., 2024).

5.3 Defect-Mediated Catalytic Electronics and Energy Conversion

The interaction between electronic structure and defect chemistry extends beyond digital computation into catalytic electronics and energy conversion. In delafossites ($CuCoO_2$) and rare-earth high-entropy perovskites, engineered point defects function as active electrochemical centers (Muhammad et al., 2024).

During oxygen evolution (OER) and hydrogen evolution (HER) reactions, surface oxygen vacancies ($V_{\ddot{O}}$) shift the local d-band energy relative to the Fermi level. Tuning d-band occupancy balances intermediate adsorption energies (∗ OH, ∗ O, ∗ OOH), lowering electrochemical reaction overpotentials. High-entropy oxide structures stabilize these defective active sites across extended operational cycles, yielding sustained catalytic activity and corrosion resistance (Pastor et al., 2022).

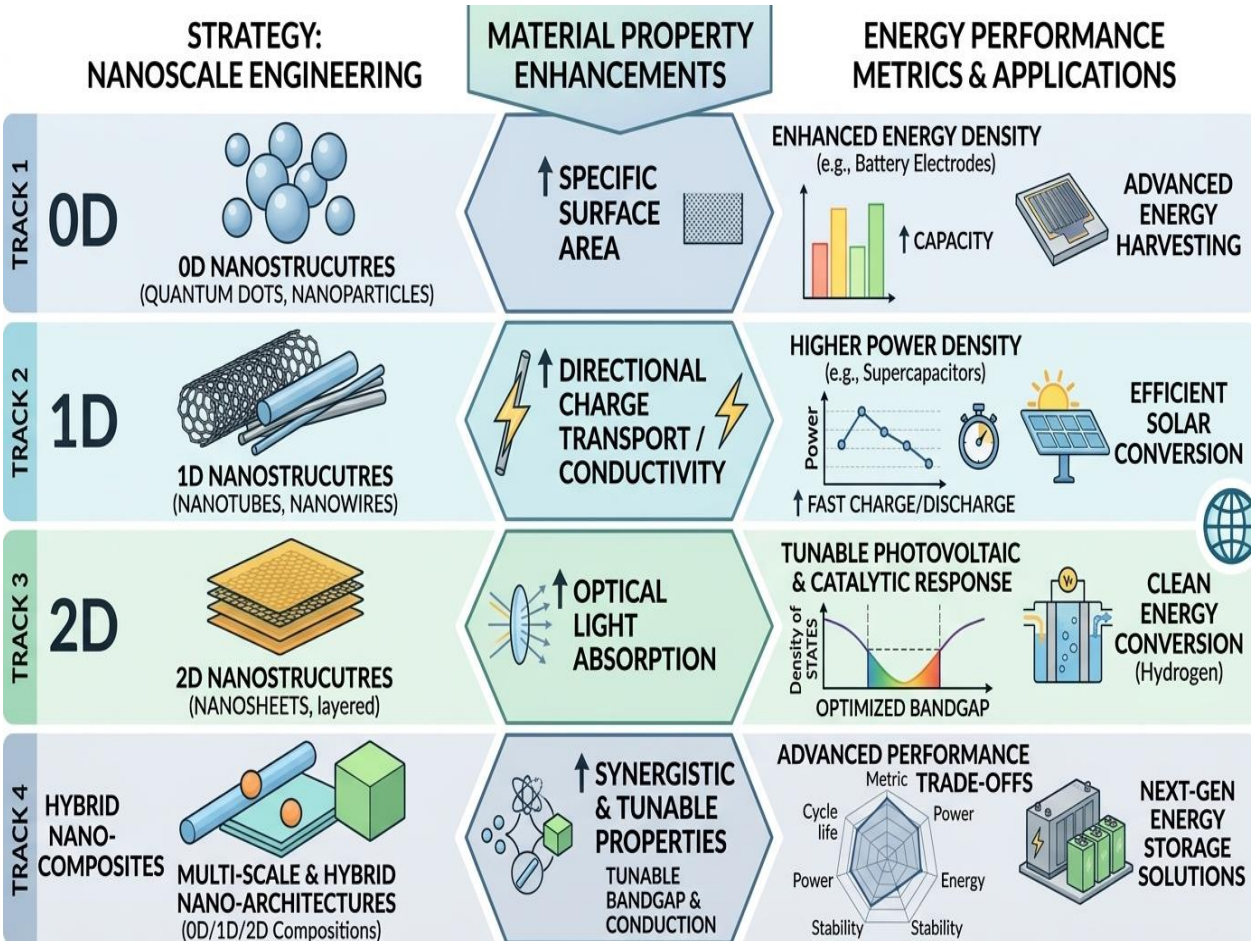


Figure 2: Multi-Track Nanoscale Engineering Strategies, Material Property Enhancements, and Energy Performance Metrics across Dimensionalities (0D, 1D, 2D, and Hybrids)

Table 3: Multi-Scale Computational and Experimental Characterization Frameworks

Scale / Domain	Modeling or Experimental Technique	Target Physical Parameters and Insights	Key Applied Research Findings
Atomistic DFT	First-principles DFT, Hubbard U corrections, Spin-Orbit Coupling.	Band structure, formation energies of point defects ($V_O^{\cdot\cdot}, V_{Cu}'$), spin topology.	Identified 2p-4f band gap shifts in ceria and anti-site defect topology in $MnSb_2Te_4$.
Quantum Non-Equilibrium Transport	DFT-NEGF, Auxiliary Mode Transient Method.	Transmission spectra T(E), conductance quantization, transient sub-picosecond current response.	Resolved anisotropic transport across grain boundaries and THz-STM transient pulse dynamics.
Semiclassical & Electro-Magnetic	3D HFSS Solvers, Hashin-Shtrikman Bounds.	Macroscopic Hall tensor $\bar{\sigma}_{xy}$, domain wall scattering, high-frequency RF response.	Differentiated intrinsic topological Hall signatures from domain-wall-induced transport anomalies.
Operando / Atomic Characterization	THz-STM, Atomic-Resolution STEM-EELS, Operando PXRD.	Sub-nm local density of states (LDOS), local Mn valence reduction, defect phase transitions.	Visualized Berry phase oscillations in LDOS; mapped $V_O^{\cdot\cdot}$ profiles at dislocation cores.

6. Emerging Bottlenecks, Synthesis Challenges, and Future Directions

6.1 Deterministic Defect Synthesis and Phase Stability

Despite theoretical progress, controlling defect formation during scalable synthesis remains a challenge. Standard chemical vapor deposition (CVD) and physical vapor deposition (PVD) growth processes often yield stochastic point defect distributions, uncontrolled grain boundaries, and chemical non-stoichiometry (Yang et al., 2026). In 2D MXenes, ambient edge oxidation degrades transport properties over time, highlighting the need for stable surface passivation strategies. Achieving sub-nanometer control over defect placement such as positioning individual nitrogen scatterers or single-atom dopants requires advanced ion implantation and atomic-layer growth protocols (Arun et al., 2025).

6.2 Artificial Intelligence and Machine-Learning-Assisted Material Discovery

Navigating multi-element chemical spaces such as high-entropy oxides and van der Waals heterostructures requires integrating artificial intelligence (AI) and machine learning (ML) with high-throughput ab initio calculations (Gao et al., 2024). Generative ML models and graph neural networks can predict point-defect formation energies, phase stability, and electronic band structures across unexplored compositional spaces. Coupling predictive computational workflows with automated synthesis platforms accelerates the discovery of optimal functional materials (Raccuglia et al., 2016).

6.3 Interfacial Strain Management and System Integration

Integrating non-silicon quantum materials into standard CMOS fabrication lines introduces challenges in strain management and defect propagation. Interfacial stress between complex oxides and silicon substrates can generate threading dislocations and interface traps, degrading carrier mobility. Addressing these integration bottlenecks requires buffer layer engineering, low-thermal-budget synthesis, and ultra-thin van der Waals dielectric encapsulation (Trung et al., 2025).

Conclusion

This review has established a comprehensive framework for quantum materials engineering by linking electronic structure, defect chemistry, and nanoscale transport dynamics as an interconnected triad governing functional material behavior. The transition from viewing crystal defects as detrimental anomalies to utilizing them as deterministic design tools represents a fundamental paradigm shift in materials engineering. Through Kröger-Vink formalisms, strain-defect coupling at dislocation cores, anti-site defect control in magnetic topological materials, and entropy-stabilized defect landscapes, we have demonstrated that point defects, vacancies, and structural boundaries can be precisely engineered to modulate electronic density of states, break inversion symmetry, induce localized magnetic order, and alter topological phase stability. Electronic structure modulation through strain engineering, moiré superlattice formation, and interfacial quantum confinement provides controllable platforms for realizing strongly correlated states, topological protection, and Rashba spin-orbit coupling. Concurrently, advanced quantum transport formalisms particularly DFT-NEGF and auxiliary-mode transient methods enable atomic-scale modeling of transmission spectra, anisotropic grain boundary transport, and sub-picosecond terahertz-driven dynamics. These theoretical advances, coupled with experimental techniques such as THz-STM and atomic-resolution STEM-EELS, bridge the gap between fundamental physics and practical device implementation. Next-generation device architectures leveraging topological surface states, spin-momentum locking, and hole spin qubits in Group-IV semiconductors demonstrate viable pathways toward ultra-low-power spintronic logic, scalable quantum processors, and defect-mediated catalytic electronics. However, realizing these applications requires overcoming critical bottlenecks in deterministic defect synthesis, scalable growth of defect-free 2D materials, and interfacial strain management for CMOS-compatible integration. Artificial intelligence and machine-learning-assisted discovery, combined with high-throughput ab initio calculations and automated synthesis platforms, offer promising solutions for navigating complex multi-element compositional spaces. Ultimately, the rational design of quantum materials hinges on a holistic understanding of how synthesis thermodynamics, defect kinetics, and quantum transport phenomena collectively determine macroscopic functionality. By integrating predictive computational workflows with precision experimental characterization and advanced fabrication protocols, the field is poised to deliver transformative technologies that transcend the limitations of classical silicon-based electronics, ushering in an era of quantum-engineered devices for computation, memory, sensing, and energy conversion.

REFERENCES

Abbas, G., Li, Y., Wang, H., Zhang, W. X., Wang, C., & Zhang, H. (2020). Recent advances in twisted structures of flatland materials and crafting moiré superlattices. Advanced Functional Materials, 30(36), 2000878.

Adak, P. C., Sinha, S., Agarwal, A., & Deshmukh, M. M. (2024). Tunable moiré materials for probing Berry physics and topology. Nature Reviews Materials, 9(7), 481-498.

Arun, A. P., Sreenivasan, N., Patil, J. H., Kusanur, R., Ramachandraiah, H. L., & Ramakrishna, M. (2025). Thin films for next generation technologies: a comprehensive review of fundamentals, growth, deposition strategies, applications, and emerging frontiers. Processes, 13(12), 3846.

Bak, T., Sherif, S. A., Black, D. S., & Nowotny, J. (2024). Defect chemistry of titanium dioxide (rutile). progress toward sustainable energy. Chemical Reviews, 124(21), 11848-11914.

Banerjee, N., Bell, C., Ciccarelli, C., Hesjedal, T., Johnson, F., Kurebayashi, H., ... & Kazakova, O. (2025). Materials for quantum technologies: A roadmap for spin and topology. Applied Physics Reviews, 12(4).

Campbell, A. J., Brotons-Gisbert, M., Baek, H., Vitale, V., Taniguchi, T., Watanabe, K., ... & Gerardot, B. D. (2022). Exciton-polarons in the presence of strongly correlated electronic states in a MoSe2/WSe2 moiré superlattice. npj 2D Materials and Applications, 6(1), 79.

Caviglia, A. D., Gabay, M., Gariglio, S., Reyren, N., Cancellieri, C., & Triscone, J. M. (2010). Tunable Rashba spin-orbit interaction at oxide interfaces. Physical review letters, 104(12), 126803.

Chen, A., Su, Q., Han, H., Enriquez, E., & Jia, Q. (2019). Metal oxide nanocomposites: a perspective from strain, defect, and interface. Advanced Materials, 31(4), 1803241.

Chen, C., Ding, X., Qin, J., He, Y., Luo, Y. H., Chen, M. C., ... & Pan, J. W. (2018). Observation of topologically protected edge states in a photonic two-dimensional quantum walk. Physical review letters, 121(10), 100502.

Chen, K., Shi, S., Li, Y., Heydari, E., Wang, J., Bartosiewicz, K., & Bai, G. (2025). Luminescent nano-structured semiconductor materials via doping engineering: Functional applications toward intelligent optoelectronics and photonics. Information & Functional Materials, 2(4), 306-325.

Chen, X., Gao, J., Wu, S., Huang, Z., Guo, Z., Hong, C., ... & Wu, S. (2026). Unveiling the impact of anti-site defects in magnetic transitions of few-layer MnBi2Te4 by operando heating. arXiv preprint arXiv:2602.07976.

Cheng, L., Wei, L., Liang, H., Yan, Y., Cheng, G., Lv, M., ... & Zeng, C. (2017). Optical manipulation of Rashba spin–orbit coupling at SrTiO3-based oxide interfaces. Nano letters, 17(11), 6534-6539.

Culcer, D., Hu, X., & Das Sarma, S. (2009). Dephasing of Si spin qubits due to charge noise. Applied Physics Letters, 95(7).

Fang, Y., Philippopoulos, P., Culcer, D., Coish, W. A., & Chesi, S. (2023). Recent advances in hole-spin qubits. Materials for Quantum Technology, 3(1), 012003.

Gao, L., Lin, J., Wang, L., & Du, L. (2024). Machine learning-assisted design of advanced polymeric materials. Accounts of Materials Research, 5(5), 571-584.

Guo, Y., Dai, B., Peng, J., Wu, C., & Xie, Y. (2019). Electron transport in low dimensional solids: a surface chemistry perspective. Journal of the American Chemical Society, 141(2), 723-732.

Ho, I. L. (2020). Excitation transport in quasi-one-dimensional quantum devices: a multiscale approach with analytical time-dependent non-equilibrium Green's function. Journal of Physics: Condensed Matter, 32(7), 075901.

Hu, X., & Das Sarma, S. (2006). Charge-fluctuation-induced dephasing of exchange-coupled spin qubits. Physical review letters, 96(10), 100501.

Hu, X., He, X., Guo, Z., Kamiya, T., & Wu, J. (2024). Antisite-defects control of magnetic properties in MnSb2Te4. ACS nano, 18(1), 738-749.

Huang, D., Choi, J., Shih, C. K., & Li, X. (2022). Excitons in semiconductor moiré superlattices. Nature nanotechnology, 17(3), 227-238.

Kemp, D. (2023). Computational studies of defect formation and migration in complex oxides under high electric fields (Doctoral dissertation, Dissertation, RWTH Aachen University, 2023).

Kim, J. M., Haque, M. F., Hsieh, E. Y., Nahid, S. M., Zarin, I., Jeong, K. Y., ... & Nam, S. (2023). Strain engineering of low-dimensional materials for emerging quantum phenomena and functionalities. Advanced Materials, 35(27), 2107362.

Kleemann, W. (2007). Universal domain wall dynamics in disordered ferroic materials. Annu. Rev. Mater. Res., 37(1), 415-448.

Kužel, P., & Němec, H. (2020). Terahertz spectroscopy of nanomaterials: a close look at charge-carrier transport. Advanced Optical Materials, 8(3), 1900623.

Lesne, E., Fu, Y., Oyarzún, S., Rojas-Sánchez, J. C., Vaz, D. C., Naganuma, H., ... & Vila, L. (2016). Highly efficient and tunable spin-to-charge conversion through Rashba coupling at oxide interfaces. Nature materials, 15(12), 1261-1266.

Liu, Y., Guan, S., Luo, J. W., & Li, S. S. (2024). Progress of Gate-Defined Semiconductor Spin Qubit: Host Materials and Device Geometries. Advanced Functional Materials, 34(19), 2304725.

Lyu, Z., Wang, Y., Sun, Y., & Dai, Y. (2026). Nanostructured high-entropy oxides for catalysis: linking entropy to function. Nanoscale, 18(15), 7825-7848.

Mengesha, W. G., & Nagessar, K. (2025). A critical review on electronic materials properties and multifunctional applications. Discover Materials, 6(1), 38.

Muhammad, P., Zada, A., Rashid, J., Hanif, S., Gao, Y., Li, C., ... & Wang, Y. (2024). Defect engineering in nanocatalysts: from design and synthesis to applications. Advanced Functional Materials, 34(29), 2314686.

Murthy, P. R., Salkar, K., Chopdenkar, P., & Durbhatkar, O. (2026). Structure–property correlations in neodymium-doped Sr2ZnTeO6: insights into optical and dielectric analysis. Journal of Materials Science: Materials in Electronics, 37(4), 342.

Pal, A., Zhang, S., Chavan, T., Agashiwala, K., Yeh, C. H., Cao, W., & Banerjee, K. (2023). Quantum-engineered devices based on 2D materials for next-generation information processing and storage. Advanced Materials, 35(27), 2109894.

Pastor, E., Sachs, M., Selim, S., Durrant, J. R., Bakulin, A. A., & Walsh, A. (2022). Electronic defects in metal oxide photocatalysts. Nature Reviews Materials, 7(7), 503-521.

Pourfath, M. (2014). The non-equilibrium Green's function method for nanoscale device simulation (Vol. 3). Vienna: Springer.

Raccuglia, P., Elbert, K. C., Adler, P. D., Falk, C., Wenny, M. B., Mollo, A., ... & Norquist, A. J. (2016). Machine-learning-assisted materials discovery using failed experiments. Nature, 533(7601), 73-76.

Rungger, I., Droghetti, A., & Stamenova, M. (2020). Non-equilibrium Green's function methods for spin transport and dynamics. In Handbook of Materials Modeling: Methods: Theory and Modeling (pp. 957-983). Cham: Springer International Publishing.

Shi, T., Cirac, J. I., & Demler, E. (2020). Ultrafast molecular dynamics in terahertz-STM experiments: Theoretical analysis using the Anderson-Holstein model. Physical Review Research, 2(3), 033379.

Shimazaki, Y., Schwartz, I., Watanabe, K., Taniguchi, T., Kroner, M., & Imamoğlu, A. (2020). Strongly correlated electrons and hybrid excitons in a moiré heterostructure. Nature, 580(7804), 472-477.

Smalley, C. J., Hughes, C. E., Willhammar, T., Pandya, R., Saikin, S. K., Johnstone, D. N., ... & Collins, S. M. (2026). Structural properties, polymorphism, and multiscale disorder unravel energy transport limitations in perylene diimide semiconductors. Science Advances, 12(22), eaed0037.

Squires, A. G., Kavanagh, S. R., Walsh, A., & Scanlon, D. O. (2026). Guidelines for robust and reproducible point defect simulations in crystals. Nature Reviews Materials, 1-18.

Sun, J., Liu, W., Liang, F., Liu, R., Yao, Y., Zou, Q., ... & Wang, S. (2026). Insight into high entropy compounds: advances, challenges and energy applications. Advanced Functional Materials, 36(1), e10855.

Szabó, Á. (2016). Dissipative quantum transport simulations in two-dimensional semiconductor devices from first principles (Doctoral dissertation, ETH Zurich).

Tasiu, I. A., Islam, M. P., Prity, M. K., Tasniya, N. M., Samar, D., Mariya, A. U., ... & Gao, J. W. (2025). Spintronics technology: A comprehensive review of materials, applications, and future trends. Journal of Science: Advanced Materials and Devices, 101087.

Trung, V. D., Zhao, W., Natsuki, J., Tan, J., Yang, W., & Natsuki, T. (2025). Synergistic interfacial engineering for ultrasensitive bionic tunable strain sensors with robust sensing stability and integrated thermal management. Chemical Engineering Journal, 508, 161056.

Uberuaga, B. P., Dholabhai, P. P., Pilania, G., & Chen, A. (2019). Semicoherent oxide heterointerfaces: Structure, properties, and implications. APL Materials, 7(10).

Wang, J. (2013). Time-dependent quantum transport theory from non-equilibrium Green's function approach. Journal of Computational Electronics, 12(3), 343-355.

Weber, B., Fuhrer, M. S., Sheng, X. L., Yang, S. A., Thomale, R., Shamim, S., ... & Nadeem, M. (2024). 2024 roadmap on 2D topological insulators. Journal of Physics: Materials, 7(2), 022501.

Yang, J., Han, J., Suo, Z., Sang, C., Yu, Y., Xin, Y., ... & Wang, L. (2026). Atomic-level precision synthesis and dynamic structure–property relationships of high-entropy nanomaterials: advances, challenges, and perspectives. Inorganic Chemistry Frontiers, 13(9), 3683-3716.

Yao, W., Aeschlimann, M., & Zhou, S. (2020). Progress on band structure engineering of twisted bilayer and two-dimensional moiré heterostructures. Chinese Physics B, 29(12), 127304.

Yoneda, J., Takeda, K., Otsuka, T., Nakajima, T., Delbecq, M. R., Allison, G., ... & Tarucha, S. (2018). A quantum-dot spin qubit with coherence limited by charge noise and fidelity higher than 99.9%. Nature nanotechnology, 13(2), 102-106.

Youssef, M., & Yildiz, B. (2012). Intrinsic point-defect equilibria in tetragonal ZrO 2: Density functional theory analysis with finite-temperature effects. Physical Review B Condensed Matter and Materials Physics, 86(14), 144109.

Zhang, X., Lu, J., Liu, J., Sun, M., Zhang, G., Kong, S., ... & Shi, X. (2026). Curvature geometry–spin electronics–catalytic dynamics coupling in emerging catalytic engineering. Chemical Society Reviews, 55(5), 2691-2730.

Zhang, Z., Wang, Y., Guo, T., & Hu, P. (2025). The influence of defect engineering on the electronic structure of active centers on the catalyst surface. Catalysts, 15(7), 651.

IEER
Institute for Excellence in Education & Research